Chapter 3

# LED and Phototransistor Simulation

Sergey Yurchuk, Oleg Rabinovich and
Sergey Didenko

Additional information is available at the end of the chapter

http://dx.doi.org/10.5772/intechopen.69629

**Abstract**

Optoelectronics (e.g., light-emitting diodes, photodetectors) is one of the most widely used fields nowadays. But it is still necessary to improve their characteristics for using in general lighting. In this chapter, the heterostructure conductivity type, impurity and indium atoms influence on the LEDs and phototransistor characteristics are investigated by computer simulation. It was found that current-voltage characteristic and quantum efficiency depend on impurity and indium atoms change a lot. By varying impurity and indium atom concentration, controlling their distribution in InGaN and AlGaP heterostructure LEDs and photodetector characteristics can be improved.

**Keywords:** light-emitting diode, InGaN, simulation, photodetector, phototransistor, AlGaP

## 1. Introduction

The ancients said: "Per crucem ad lucem" ("Through the cross to the light"). Another field of modern science and technology could be hardly remembered, which has influenced economics and science so greatly as semiconductor devices, especially optoelectronics. Such devices have a very fascinating history. The optoelectronics started at the beginning of the twentieth century, and its progress was so dynamic that it can be compared with the modern scientific and technological revolution.

Below, valuable steps of optoelectronics development should be briefly pointed out. In 1907, a captain Henry Joseph Round (**Figures 1** and **2**), personal assistant to Guglielmo Marconi, took a piece of carborundum and saw the yellow light by applying voltage to this material, but he in the paper described only experiment without any physical explanation of this phenomenon [1–4].

**Figure 1.** Henry Joseph Round.

## A Note on Carborundum.

*To the Editors of Electrical World:*

SIRS:—During an investigation of the unsymmetrical passage of current through a contact of carborundum and other substances a curious phenomenon was noted. On applying a potential of 10 volts between two points on a crystal of carborundum, the crystal gave out a yellowish light. Only one or two specimens could be found which gave a bright glow on such a low voltage, but with 110 volts a large number could be found to glow. In some crystals only edges gave the light and others gave instead of a yellow light green, orange or blue. In all cases tested the glow appears to come from the negative pole, a bright blue-green spark appearing at the positive pole. In a single crystal, if contact is made near the center with the negative pole, and the positive pole is put in contact at any other place, only one section of the crystal will glow and that the same section wherever the positive pole is placed.

There seems to be some connection between the above effect and the e.m.f. produced by a junction of carborundum and another conductor when heated by a direct or alternating current; but the connection may be only secondary as an obvious explanation of the e.m.f. effect is the thermoelectric one. The writer would be glad of references to any published account of an investigation of this or any allied phenomena.

NEW YORK, N. Y. H. J. ROUND.

**Figure 2.** H.J. Round's paper.

http://dx.doi.org/10.5772/intechopen.69629

Oleg Vladimirovich Losev's first papers were at the beginning of the twentieth century.

O.V. Losev investigated and carried out physical explanation for injectional and prebreakdown luminescence effects in details [2–6]. Even more, O.V. Losev received first patent for presample of light-emitting diode (LED) in 1927 (**Figures 3** and **4**).

As it was written by Egon E. Loebner upto 50th year, such effects were called "Losev light" [3]. First contemporary explanation of p-n junction lighting effect was proposed by Kurt Lehovec et al. from Signal Corps Engineering Laboratories (New Jersey) in 1951. In the 1960s, the first GaAs-based near-infrared semiconductor lasers and red-orange light-emitting diodes were introduced by Nick Holonyak and Mary George Craford. In parallel to that development, photodetectors based on III–V semiconductors were developed [4, 7]. In 1963, Zhores Ivanovich Alferov proposed the idea of using nanoheterojunctions (NH) in emitters (**Figure 5**).

Under Alferov leadership, GaAs-AlGaAs heterojunction investigations were carried out [5, 8, 9]. In 1966, for the first time, effective radiative recombination at p-n junction of four-component solid solution $As_xP_{1-x-y}GaIn_y$ was discovered. In 1970, Zh. I. Alferov et al. proposed to use four-component structure for achieving heterojunctions. In 1966, N. Holonyak presented epitaxial growth process [8, 10]. In 1969, Herbert Paul Maruska and James J. Tietjen grew the first GaN

**Figure 3.** Oleg Vladimirovich Losev.

Класс 21 а, 27 № 12191

# ПАТЕНТ НА ИЗОБРЕТЕНИЕ

## ОПИСАНИЕ

### светового реле.

К патенту О. В. Лосева, заявленному 28 февраля 1927 года (заяв. свид. № 14672).

О выдаче патента опубликовано 31 декабря 1929 года. Действие патента распространяется на 15 лет от 31 декабря 1929 года.

Предлагаемое изобретение использует общеизвестное явление свечения в карборундовом детекторе и состоит в том, что в световом реле для быстропишущего телеграфного или телефонного приема, передачи изображений на расстояние и других целей, в качестве модулируемого электрическим током источника света, применяется свечение в точке контакта карборундового детектора, включенного непосредственно в цепь модулирующего тока.

На чертеже фиг. 1 изображает схему предлагаемого светового реле и фиг. 2—схему устройства для фотографической записи сигналов с применением светового реле.

К зажимам *A* источника тока сигналов, подлежащих записи, через потенциометр *P* включается светящийся карборундовый детектор *D*, в цепь которого включена батарея *B*, дающая дополнительное постоянное напряжение для наложения его на напряжение тока сигналов и усиления действия реле; путем регулировки этой батареи создаются наивыгоднейшие условия работы детектора *D*. Оптическая система *L* предназначена направлять световой поток, излучаемый карборундовым детектором, на движущуюся фотографическую пластинку *F*, на которой производится запись изменений этого потока. Детектор *D*, оптическая система *L* и пластина *F* заключены в светонепроницаемую камеру. Примерное включение светового реле показано на чертеже 2, где *E* — приемник-усилитель высокой частоты, *T* — автотрансформатор высокой частоты, а остальная часть схемы аналогична только-что описанной.

### Предмет патента

1. Световое реле для быстропишущего телеграфного или телефонного приема, передачи изображений на расстояние и для других целей, характеризующееся применением, в качестве модулируемого электрическим током источника света, свечения в точке контакта карборундового детектора общеизвестного устройства, каковой детектор включен непосредственно в цепь модулирующего тока.

2. Видоизменение охарактеризованного в п. 1 светового реле, отличающееся тем, что последовательно с указанным детектором *D* включен источник дополнительного напряжения постоянного тока *B* (фиг. 1 и 2) с целью усиления действия реле.

**Figure 4.** O.V. Losev's patent for preLED.

single crystal on a $Al_2O_3$ by hydride vapor phase epitaxy. The first bluish-green LED having a metal-insulator-semiconductor (MTS) structure was developed by Jacques I. Pankove et al. in 1971. In 1985, Isamu Akasaki and Hiroshi Amano et al. succeeded in growing extremely high-quality GaN with a surface on a sapphire substrate by pioneering a low-temperature-deposited (LT) buffer layer technology using organometallic vapor phase epitaxy (OMVPE). In 1989, they achieved fixing Mg concentration in the GaN growth by OMVPE using $Cp_2Mg$. Then, first, they discovered distinctly p-type GaN with low resistance by low-energy electron-beam irradiation (LEEBI) on high-quality Mg-doped GaN grown with the LT-buffer layer, which lately led to the creation of high-efficiency LEDs. They and Shuji Nakamura demonstrated the first p-n junction UV (edge emission) and violet LED and also achieved p-type AlGaN in 1991 and p-type GalnN in 1994, accordingly [2, 10–13].

**Figure 5.** Zhores Ivanovich Alferov.

Quantum-sized semiconductors used in photonics and optoelectronics (e.g., light-emitting diodes, lasers, photodetectors, etc.) are AIIIBV and AIIBVI N. Their solutions are very interesting due to their unique properties—the wide band gap, strong bonds, and high thermal conductivity. The main outstanding properties of nitride heterostructures are forbidden gap energy that depends on the indium concentration and could change in the range 1.95–6.3 eV. AlGaInN has very bright future in various applications fields—short-wavelength electroluminescence and high-power/temperature/frequency electronic devices. Now, problem of limited color range and lack of high-power white LEDs that previously prevented LED usage for general lighting have been solved. Unfortunately, there are still several problems need to be solved, e.g., LED degradation, efficiency droop nature understanding, quantum efficiency (QE) increase, obtaining optimal quantum size area structure, photodetectors efficiency increase, and developing the method for quick NH and device investigation.

For complex materials and optoelectronic devices, the basic factors that determine their quality, such as current-voltage characteristics (I-V) and the efficiency, can be investigated by computer simulations and include taking into account major structural and physical NH and device parameters [15–24].

## 2. Simulation basis

For complex materials and optoelectronic devices, the basic factors that determine their quality, such as I-V characteristics and the efficiency, can be investigated by computer simulations

that include taking into account major structural and physical NH and device parameters [14–23]. The last decade proved an increased usage of the software for simulation semiconductor devices. Device simulations play an important role in their research. The formulas for devices are complicated. The growth process was simulated, and light propagation and extraction, and the possibility of the external efficiency increase of AlGaInN LED were studied by simulation; explanation of the electroluminescence efficiency degradation at increasing current was suggested.

Freeware computer program SimWindows was used in our investigation [14]. The specific features of this program are: (1) the electrical, optical, and thermal device properties for simulation based on system of exact physical equations, (2) the simulation possibilities with different approximations for two-lead devices and (3) the quantum-sized device simulation. The software extends a lot of traditional electrical models by adding effects such as quantum confinement, tunneling current, and complete Fermi-Dirac statistics. The optical model includes computing electromagnetic field reflections at interfaces. The software is very flexible for semiconductor device simulation. Exact solutions of electrical, optical, and heat transport phenomena in 1D situation are included. For example, drift-diffusion currents, thermoionic and tunneling currents for electrons and holes are taken into account, and in recombination of charge carriers, radiating and nonradiating are included. For band diagram calculations of devices, Fermi-Dirac or Boltzmann statistics and full version of Poisson differential equation have been used. During our investigation, special files for NH, photodetectors, and LED simulations were created. Of course, piezoelectric and spontaneous effects were additionally taken into consideration by including piezo and elastic matrix coefficients. The main parameters for NH, photodetector, and LED type were included into the individual, relating each device and material, special files for simulation. In those files, parameters such as geometric sizes for emitters, QW, and barriers; the QW and barriers quantity; the solid solution content; the conductivity type; and doping concentrations were included. In the materials file for heterostructures, more than 25 parameters such as the band gap, refractive index, optical absorption, thermal conductivity, mobility, and lifetime of charge carriers, and the coefficients of radiative and nonradiative recombination were included. Initial data-preparing files were based on Refs. [24–30].

## 3. Light-emitting diode improvements

One of the most important parameters that describe LED is the QE ($\eta_{QE}$). By definition, QE is equal to the sum of the radiative and nonradiative recombination rates. If the NH active area is a QW set with the equal length, the QE expression (Eq. (1)) is:

$$\eta_{QE} = \frac{\sum U^k_{B-B}}{\sum U^k_{Total}}, \tag{1}$$

where $k$ is the QW number from 1 to $m$.

Understanding the QE dependence according to different influence is very useful for predicting the NH and LED reliability.

Blue InGaN NH contained, n-GaN-emitter ($N_D = 10^{19}$ cm$^{-3}$), in active area were QW and GaN-$In_{0.2}Ga_{0.8}N$ barriers. The QW quantity varied from 1 to 5. In the first group of simulated NH, the QW width was 2 nm and the GaN-barrier was 3 nm, whereas 3.5 and 4.5 nm in the second group. For each QW set, three types of devices with different doping QW and barriers were simulated: i-type, n-type (the ionized concentration was $N_D = 10^{18}$ cm$^{-3}$), and p-type ($N_A = 10^{18}$ cm$^{-3}$); for the p-GaN-emitter, the (Mg) acceptor concentration was $N_A = 10^{18}$ cm$^{-3}$; green InGaN LEDs were identical in parameters to blue ones except for the QW structure—$In_{0.35}Ga_{0.65}N$. Red AlGaInP NH had the following structure: n-$Al_{0.4}Ga_{0.1}In_{0.5}P$-emitter, the donor concentration was $N_D = 10^{18}$ cm$^{-3}$; the active area consisted of QW and $Ga_{0.5}In_{0.5}P/Al_{0.1}Ga_{0.4}In_{0.5}P$ barrier set. The QW quantity varied from 1 to 10. In the first group of NH, the QW width was 2 nm and the barrier width was 3 nm, while 3.5 nm and 4.5 nm in the second group, 10 nm and 10 nm in the third group and 50 nm and 50 nm in the fourth group. NH simulation was carried out with doping QWs and barriers with an acceptor impurity (Zn) $N_A = 5 \times 10^{17}$ cm$^{-3}$, while for the p-$Al_{0.4}Ga_{0.1}In_{0.5}P$-emitter, the acceptors (Zn) were $N_A = 5 \times 10^{17}$ cm$^{-3}$. In the case of the yellow AlGaInP, the NH was identical to the red one $Al_{0.17}Ga_{0.33}In_{0.5}P$, and the barriers were $Al_{0.4}Ga_{0.1}In_{0.5}P$. LED simulation was performed at 100 A/cm$^2$ and at a temperature of 300 K.

In **Figure 6**, it could be seen as main characteristics that could be done during simulation, e.g., InGaN heterostructure. The dependence for main parameters vs. voltage is shown below.

With applying no voltage, electrons and holes are mainly concentrated in n- and p-type areas, respectively, and after applying voltage, they are redistributed into the middle QWs (**Figure 6**). Basic dependence trend of simulation results blue/green LED (**Figure 7**). Based on the results, it can be seen that the most economically sound and effective (based upon internal quantum efficiency) production is LEDs with 4 QWs (3.5 nm width). It is due to LED with 4 QWs, the internal quantum efficiency is maximum, and at the same time, resistance is not at its maximum value.

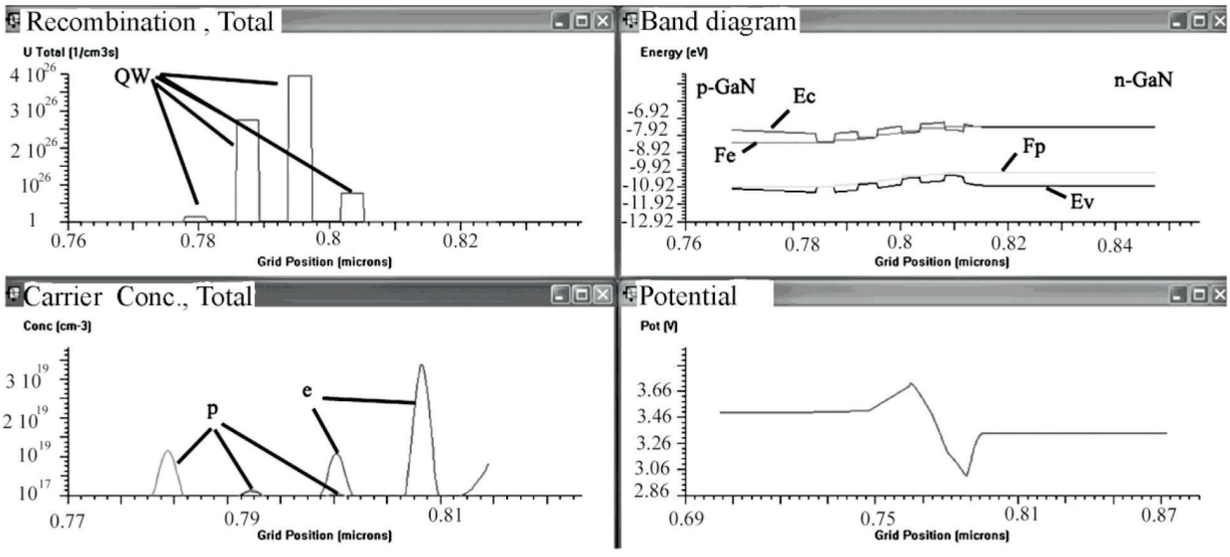


**Figure 6.** Basic characteristics.

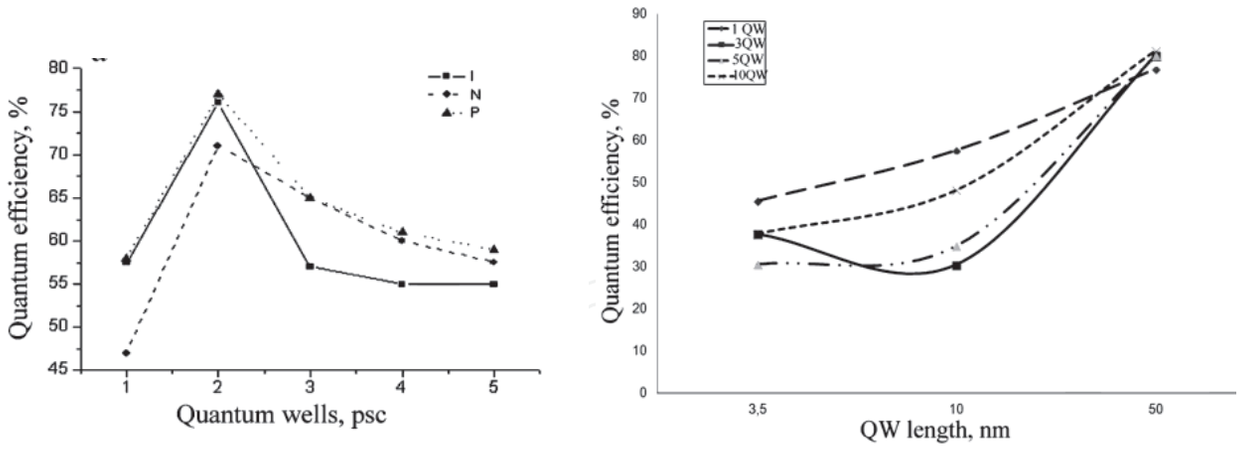


**Figure 7.** Internal quantum efficiency for nitride (left) and phosphide (right) LED per QW quantity (QW 3.5 nm) at 100 A/cm$^2$.

The maximum QE was in the central QWs. It is detected that the active region should contain 4 QWs (central ones are according to recombination and edge concentrate carrier currents for a higher recombination). In red and yellow NH (**Figure 7**, right), the QE increase at different QW width is observed. Maximum QE occurs at QW width—50 nm. For yellow NH, the QE was three times less than in the red one. The difference is because of reducing the radiative recombination efficiency and small energy gap between the G- and X-minimum in the conduction band.

Now, let us discuss on the investigation including green and blue InGaN LEDs simulation with different indium atom concentration for blue $X$ = 0.15 – 0.25 and green $X$ = 0.25 – 0.35. In published experimental works, it was detected that in $In_XGa_{1-X}N$ quantum, well-active region of blue and green LED spatial indium content fluctuations are responsible for many peculiarities of electrical and optical characteristics of devices. In Refs. [31, 32], the idea was given that QW area in blue and green LEDs should be described as a combination of spatially distributed regions which have their own fixed indium atom concentration. In such description, each small area can be as a local NanoLED, which has its own p-n junction area. In general, the LED = NanoLEDs sum with the electrical parallel connection. In our theoretical calculations, it was proposed to use Gauss distribution function for calculations of "NanoLED" p-n junction areas. In this case, the area $S(x)$ for each indium content $x$ is described by expression (Eq. (2)):

$$S(x) = 10^{-2} S_{LED} 1/[\sigma * (2\pi)^{0.5}] * \exp - \left\{ \left(x - x_0\right)^2 / 2\,\sigma^2 \right\}, \quad (2)$$

where NanoLED—LED p-n junction area, $x_0$—indium content value.

It was supposed that, for blue LED, indium concentration varies $X$ = 0.15 – 0.25 and $X_0$ = 0.20. In this situation, $\sigma$ = 0.017 to have fulfillment of the "3 $\sigma$" rule, providing 0.999 reliability of calculations. The Gauss distribution of $S(x)/S_{LED}$ values on $X$ and NanoLED connection are presented in **Figures 8** and **9**, respectively.

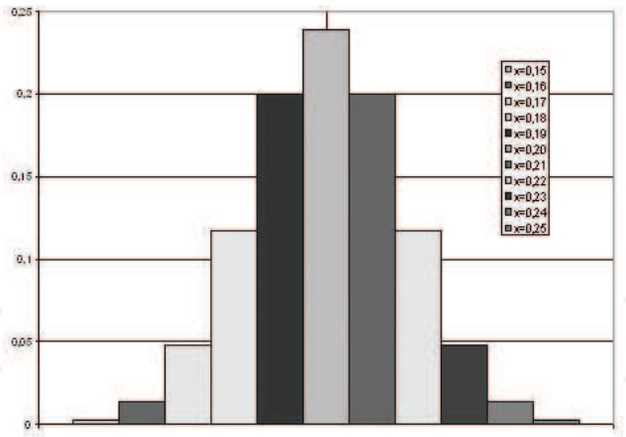


**Figure 8.** The Gauss distribution of $S(x)/S_{LED}$ values on $x$.

The current density-voltage dependences on p-n junctions having different indium content $X$ are shown in **Figure 10**.

Spectrum is with asymmetric shape. Simulation proves the "blue shift" vs. current increase even at quantum Stark-Keldysh effect neglecting is proved by the simulation (**Figure 11**).

It was detected that by In concentration changes I-V or spectrum curves could be shifted. Doping into the p-emitter of NH (e.g., $Al_{0.2}Ga_{0.8}N$) was suggested to eliminate electron injection from the active region, which is especially important in device simulation with a low content of In ($X$) atoms (**Figure 12**).

Next, on the basis of the optimized structure of the NH, the effect of the impurity and In atoms doped into the barriers between QWs in the NH active region was studied; this effect is shown by the nonideality coefficient dependence, as shown in **Figure 13**.

With no QWs in the active area ($X = 0$), the I-V has standard dependence. At low current densities, $\eta > 1$, an interesting dependence of electron and hole recombination in the space-charge

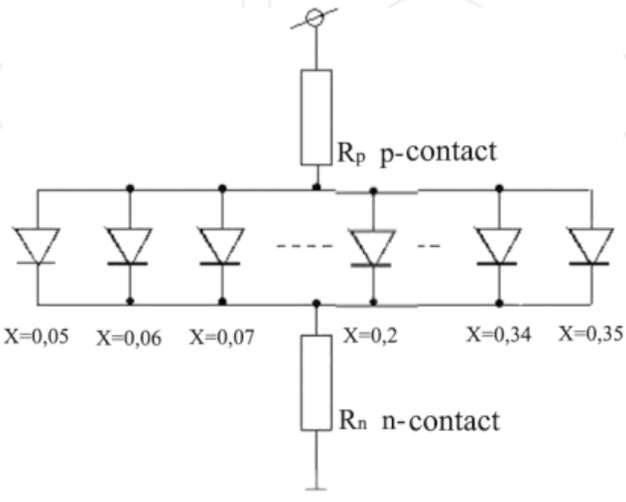


**Figure 9.** Parallel connection of nanodimensional elements (NanoLEDs).

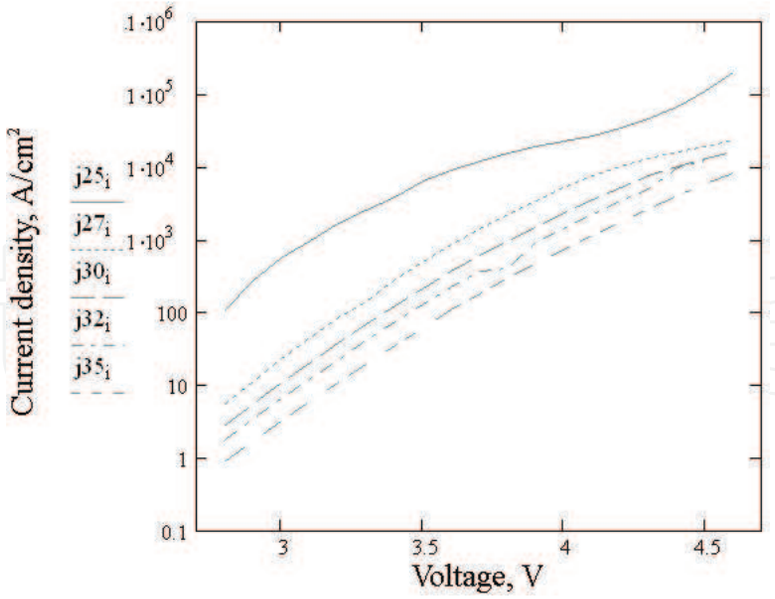


**Figure 10.** Current densities per voltage (at different In concentration $X$ = 0.25, 0.27, 0.3, 0.32, and 0.35).

region (SCR) vs. current is observed. The above barrier-current carrier injection increasingly begins to predominate at $\eta \rightarrow 1$ at a low injection level ($J$ = 1–20 A/cm$^2$) and $\eta \rightarrow 2$ with increasing injection level ($J$ = 20–500 A/cm$^2$). For $X > 0.1$, the $\eta$ increases over the range of $J$ = 0.1–500 A/cm$^2$, reaching $\eta > 2$ and even higher for $X > 0.15$. The nonideality coefficient decreases with increasing donor impurity concentration in the barrier for the same values of $X$ and $J$.

Then, the impurity influence on the I-V was studied. The optimum impurity concentration in barriers between QWs was detected at about $N_d = 10^{18}$ cm$^{-3}$, and the indium atoms concentration at 7 %. This doping shifts the I-V to the lower voltage region and increases the QE (**Figure 14**).

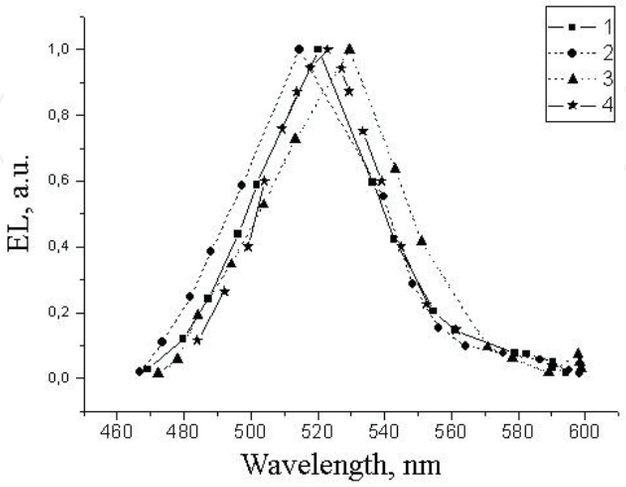


**Figure 11.** Electroluminescence spectral characteristics: 1—$X$ = 0.15, 2—$X$ = 0.20, 3—$X$ = 0.25, and 4—$X$ = 0.30.

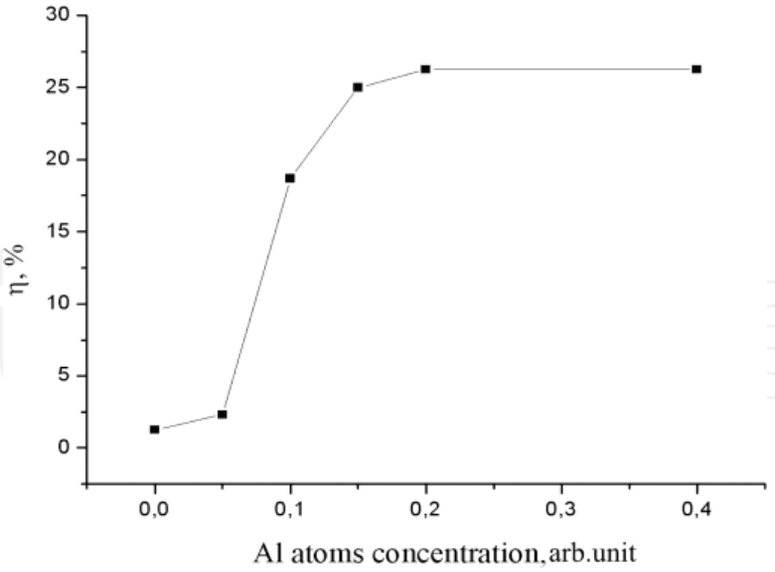


**Figure 12.** The influence of the Al atom content in p-emitter on QE.

This effect is due to potential barrier decrease between QWs and barriers among them, so $J$ increases at a constant voltage. By varying the indium atom concentration and doping concentration in the active region, we could rise QE at the same voltage. Blue LED electrical and optical parameters and characteristics vs. current density trend and temperature are proved by direct computer simulation based on the new model of a LED QW active region, having spatial indium content fluctuations: I-V characteristics. At current densities less than 1 A/cm$^2$, I-V dependences are very close. They are close to exponent dependencies $J \sim \exp(eU/nkT)$ at all $X$ and temperatures in the range of −40°C to +125°C, where $n$ is so-called nonideality factor. At higher current densities and at voltage increase, $n$-values are gradually increasing.

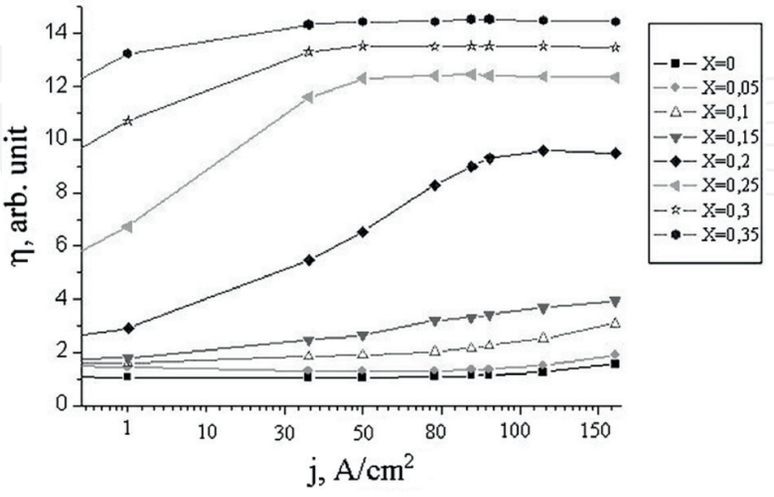


**Figure 13.** Nonideality coefficient $\eta$ vs. $j$ dependence.

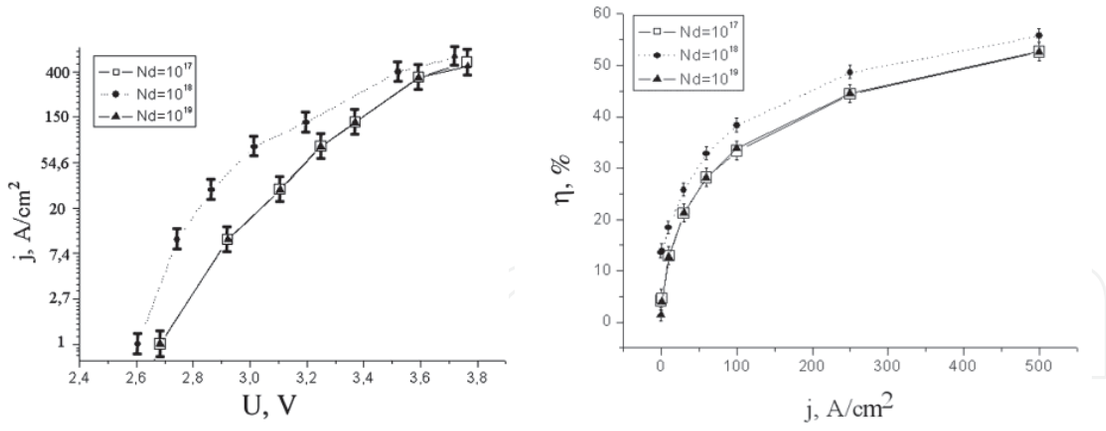


**Figure 14.** I-V, $\eta$ vs. $j$ according to barriers doping between QWs.

In **Figure 15**, satisfactory agreement between the simulation and experimental results is evident, despite the fact that the simulation results are obtained without any additional (other than those of the base physical models) approximations.

During simulation, efficiency droop was investigated too. It was detected that the injected electrons and holes are irregularly distributed in the QW. Carrier recombination is concentrated in the QW. In the active region, the local electrostatic potential change is due to the spatial of electrons and holes in active region distribution. Simulation was carried out initially at the assumption that there is little difference between the carriers' lifetime $\tau_{n0} \approx \tau_{p0} = 10^{-9}$ s, without detecting efficiency droop (**Figure 16**, curve 1).

It was suggested that there is a big difference between $\tau_{n0} = 10^{-11}$ s and $\tau_{p0} = 10^{-8}$ s, which was in correlation with the experimental results. It was detected that the capture coefficient in radiative recombination was $B = 10^{-10}$ cm$^3$/s. This significant asymmetry of carrier lifetimes is according to deep donor/acceptor levels from defects or autodoping process. Generally, this is due to indium atom redistribution in active area. AlGaInN NH were grown by MOCVD on

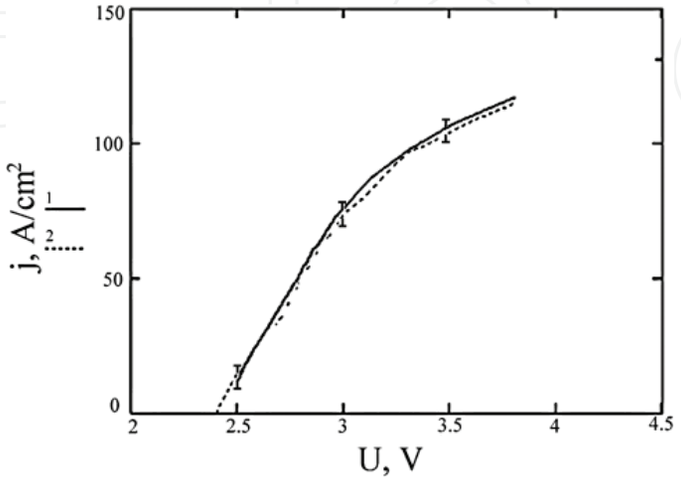


**Figure 15.** I-V LED: simulation (1) and experiment (2).

http://dx.doi.org/10.5772/intechopen.69629

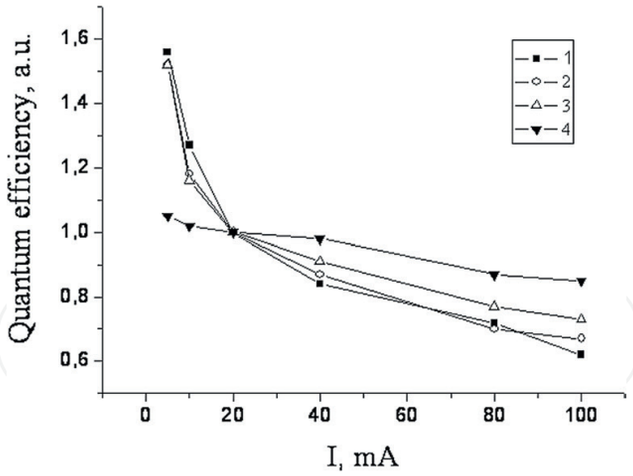


**Figure 16.** Quantum efficiency vs. current.

SiC and $Al_2O_3$ substrates after simulation suggestions. Based on growth results (e.g., photoluminescence spectral curve and Peak lambda), it was detected that the characteristics have similar trend. The spectral mapping for NH is shown in **Figure 17**.

In **Figure 17**, indium atom concentration distribution over wafer is shown. Impurity-defect cluster creates deep energy levels near the middle of the band gap, and the electron capture will be faster than the holes by the centers, due to the fact that its efficiency droop will be based on injected carrier redistribution between the QWs. For reducing droop, it needs to improve NH growth quality by usage Si (111) or better GaN substrates [33].

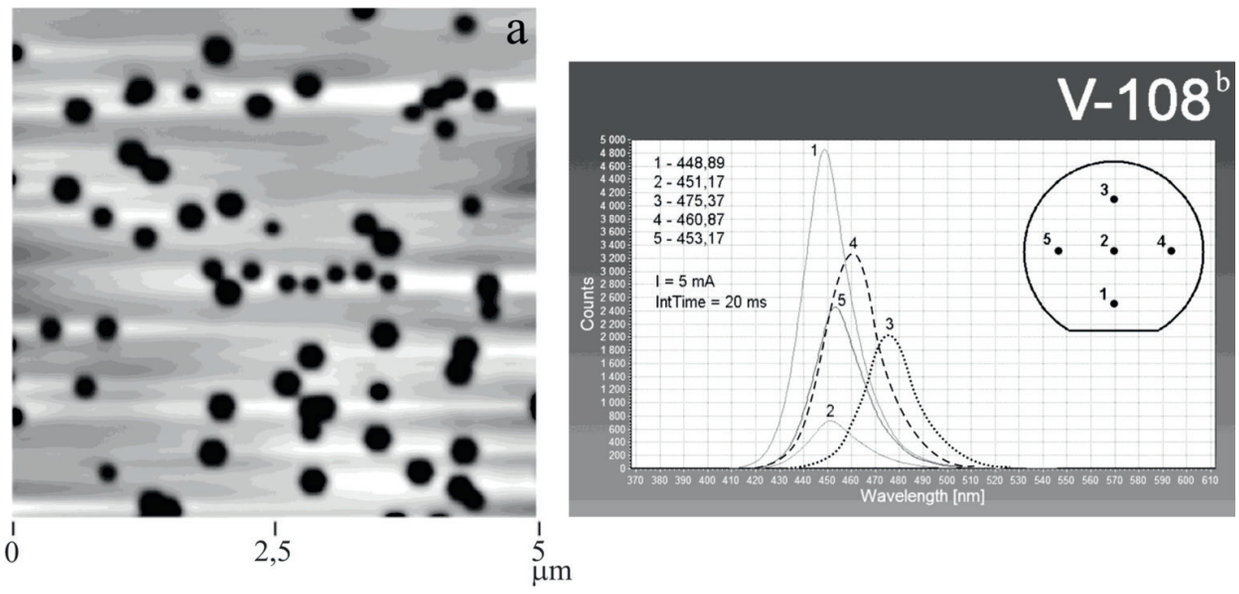


**Figure 17.** (a) AFM scan of the InGaN/GaN heterostructure with different indium concentration across active region [32]; (b) photoluminescence spectral curve and peak lambda of the InGaN/GaN heterostructure with different indium concentration across wafer.

## 4. Photodetector (phototransistor) improvements

Photodetector efficiency increase for the ultraviolet spectral range is discussed. Such devices can be widely used in various fields of technology, including devices that analyze the composition of gases and liquids, and in the open optical communication lines with increased noise immunity in high solar radiation.

One of the most promising ways to create UV photodiodes is $Al_XGa_{1-X}N$ NH usage, and the base technology of their growth is metal organic chemical vapor deposition compounds (MOCVD), which allows producing NH with high performance. Theoretically, this NH allows creating photodiodes in the wavelength range of 220–350 nm. Now, it has been developed and manufactured a photodiode AG38S-SMD with sensitivity 0.12–0.16 A/cm$^2$ for the radiation wavelength range of 250–350 nm [34].

Our investigations based on computer simulation showed that, based on such NH, not only photodiodes but also phototransistors (PT) with a sensitivity of more than 100 A/cm$^2$ can be produced, in this wavelengths area [35–43]. Ultraviolet phototransistor (UV PT) structure has been proposed, based on the capabilities of this technology with GaN and AlGaN collector. Here, the first step of the PT development is investigated, defining the multilayer NH constructor by computer simulation: the structure type (n-p-n or p-n-p), the aluminum content, dopant thickness, and concentration in the layer structure and other parameters.

For $Al_XGa_{1-X}N$ photodetector (photodiodes and phototransistors) simulation, special materials and device files were created in the same style as were previously for NH and LEDs. **Figure 18** shows the energy band diagram of a symmetric structure n-AlGaN/p-GaN/n-AlGaN.

Photodetectors are characterized by high values of gain for both shift polarities. Effective injection capacity is provided by the fact that the p-GaN base layer has a narrower band gap than the emitter and collector layers. During NH simulation for high efficiency and high sensitive phototransistor, the structure consisted of the p-$Al_{0.3}Ga_{0.7}N$ collector, n-$Al_{0.3}Ga_{0.7}N$ emitter with an aluminum content of 30% and a p-GaN base. The emitter and collector thickness was 0.875 μm, and the base thickness was 0.3 μm. Acceptor concentration in p-$Al_{0.3}Ga_{0.7}N$ collector was $10^{17}$ cm$^{-3}$, donors in n-$Al_{0.3}Ga_{0.7}N$ emitter were $10^{17}$ cm$^{-3}$ and the acceptor concentration in the p-GaN base was $10^{17}$ cm$^{-3}$ or $10^{18}$ cm$^{-3}$. The lifetime values of the nonequilibrium electrons and holes in all areas of PTs were equal to 50 ns. The device files have been created for both the concentration of acceptors in the base.

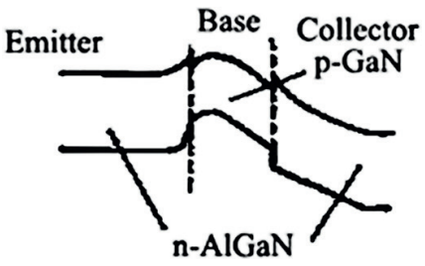


**Figure 18.** The current-voltage characteristic of a phototransistor double heterojunction.

Method for PT characteristics simulation at two acceptor concentrations in PTs base (Na = $10^{17}$ $cm^{-3}$ or Na = $10^{18}$ $cm^{-3}$) includes steps as it is shown below: (1) for the dark current density value $J_{Ph}$, A/$cm^2$ determination at different voltage $U$ between the PT emitter and collector (plus on p-$Al_{0.3}Ga_{0.7}N$ collector), the voltage range was $U$ = (1–9) V; (2) for the photocurrent density value $J_f$ determination at various lighting power density values $P$ was $P$ = ($10^{-6}$ to $10^{-1}$) W/$cm^2$ and voltage between the PT emitter and the collector (plus on p-$Al_{0.3}Ga_{0.7}N$ collector) was $U$ = (1–9) V. The energy of quanta during lighting was $E$ = 3.5 eV. The Al mole fraction in the collector and emitter was varied from $X$ = 0.2 to $X$ = 0.3.

Dark current density $J_{Ph}$ dependence at the voltage on PT is shown in **Figure 19**.

It is clearly seen that in the PTs at an acceptor concentration in the base $N_a$ = $10^{17}$ $cm^{-3}$, dark current begins to rise sharply at a voltage greater than 8 V, which obviously corresponds with start of the clamping of the emitter and collector (Early's effect). When the acceptor concentration in the base $N_a$ = $10^{18}$ $cm^{-3}$, this effect occurs at higher voltages. At voltages less than 8 V, dark current density does not exceed $10^{-8}$ A/$cm^2$. This value limits the minimum magnitude of photocurrent density and, consequently, the minimum value of the recorded radiation power. Photocurrent density $J_f$ dependence at the light power density $P$ at a constant voltage $U$ between the PTs emitter and the collector is shown in **Figures 20** and **21**. Lighting power range was $P$ = ($10^{-6}$ to $10^{-1}$) W/$cm^2$; the voltage range was $U$ = (1–9) V. Due to huge data, it is presented by three subrange voltages (1–3), (4–6), and (7–9) V.

**Figure 22** clearly shows that at the acceptor concentration in the base $N_a$ = $10^{18}$ $cm^{-3}$, the PTs sensitivity has a large value in a wide range of lighting, especially in the region of small power values $P$.

At the same time, at the acceptor concentration in the base $N_a$ = $10^{17}$ $cm^{-3}$, the PT sensitivity is maximum at relatively larger values of the power $P$, which makes them very promising in a variety of applications. **Figure 23** shows the PT sensitivity dependence at voltage in the range from 1 to 9 V at a power density of light 1 mW/$cm^2$, which is typical in many applications of UV photodetectors.

Conclusion of this dependence is quite obvious—to obtain a high sensitivity at voltage, applied to the PT, it must be in the range of 6–9 V. At the end of the discussion of UV phototransistor characteristics simulating, data of the PTs sensitivity spectral dependence are presented (**Figure 24**).

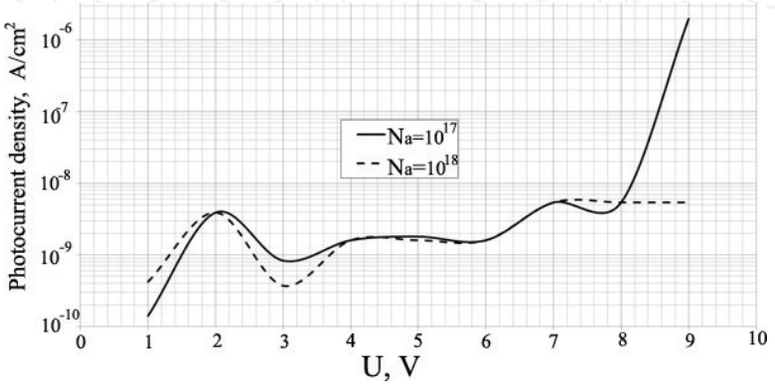


**Figure 19.** Dark current density $J_{Ph}$ vs. the PT voltage.

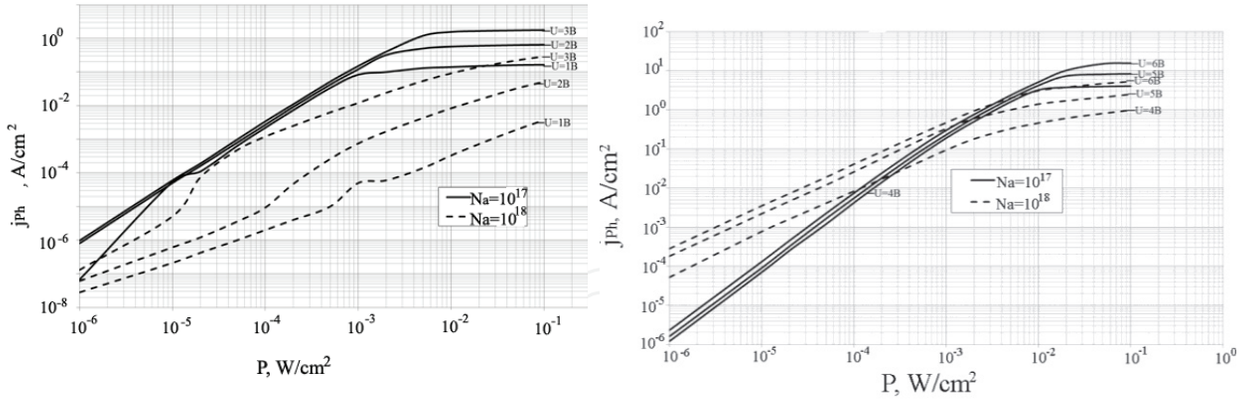


**Figure 20.** Photocurrent density $J_{Ph}$ vs. irradiation power $P$ at $U$ = 1–6 V.

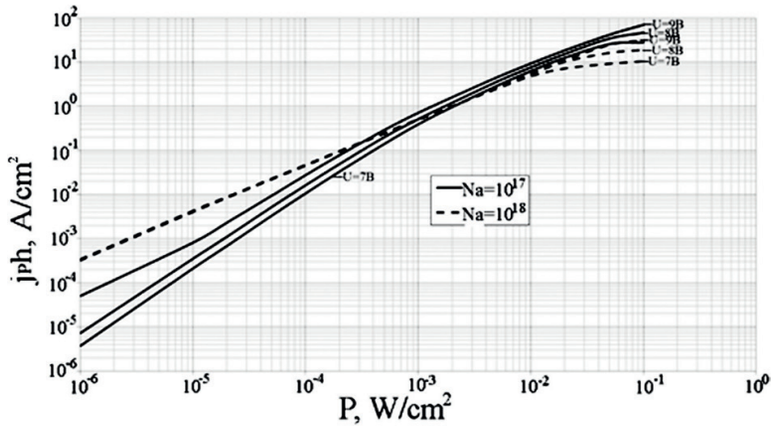


**Figure 21.** Photocurrent density $J_{Ph}$ vs. irradiation power $P$ at $U$ = 7–9 V.

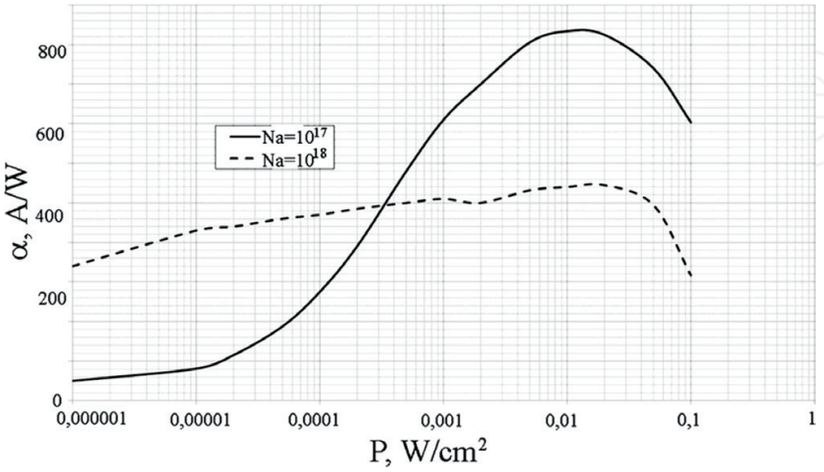


**Figure 22.** Phototransistor sensitivity vs. light power at $U$ = 9 V.

http://dx.doi.org/10.5772/intechopen.69629

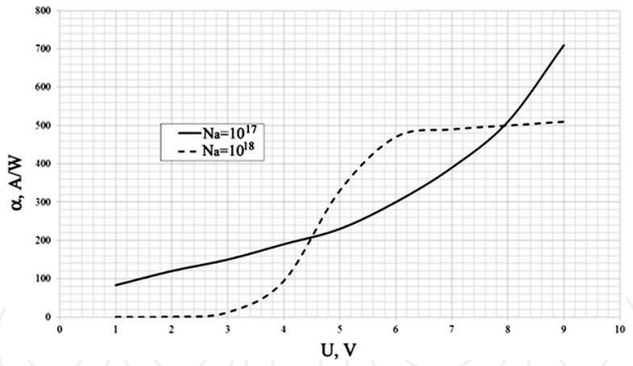


**Figure 23.** Phototransistor sensitivity vs. voltage at the power illumination density of 1 mW/cm$^2$.

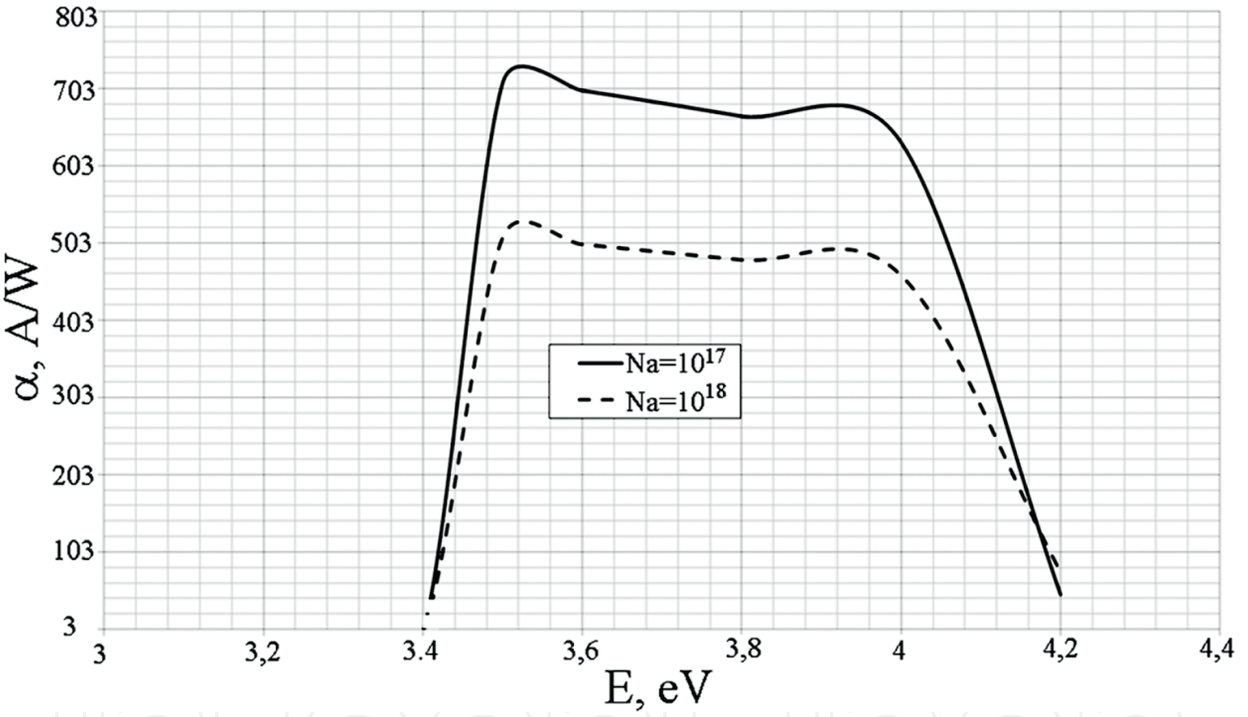


**Figure 24.** Phototransistor sensitivity vs. quanta energy $E$ at $P = 10^{-3}$ W/cm$^2$ and $U = 9$ V.

It is clearly seen that the PTs sensitivity is very high in the range of photon energies from 3.5 to 4 eV (wavelength range from 354 to 309 nm), which allows to use them as selective photodetectors. PTs selectivity can be increased by reducing the aluminum concentration in the p-$Al_{0.3}Ga_{0.7}N$ collector up to 20%. Sensitivity also can be increased by improving MOCVD technology for more high-quality AlGaN multilayer structures (with minimum defect concentration). If the sapphire substrate could be replaced by a gallium nitride substrate grown on sapphire, the lifetimes of nonradiative recombination in the PTs base will be increased significantly.

## Author details

Sergey Yurchuk, Oleg Rabinovich* and Sergey Didenko

*Address all correspondence to: rawork2008@mail.ru

The National University of Science and Technology "MISiS", Moscow, Russian Federation

## References

[1] Round HJ. A Note on Carborundum Electrical World. 1907;**49**:309

[2] Schubert EF. Light-Emitting Diodes. Cambridge: Cambridge University Press; 2006. p. 422. DOI: 0-521-01784-X

[3] Loebner EE. Subhistories of the light emitting diode. IEEE Transactions on Electron Devices. 1976;**23**:675-699. DOI: 10.1109/T-ED.1976.18472

[4] Craford MG. Visible light emitting diodes: Past, present and very bright future. MRS Bulletin. 2000:27-31. DOI: 10.1557/mrs2000.252

[5] Novikov MA. Oleg Vladimirovich Losev: Pioneer of semiconductor electronics. Soviet Physics: Semiconductors. 2004;**1**:5-9 [in Russian]

[6] Losev OV. Optical Relay. Patent No. 12 191, February 2, 1927

[7] Hangleiter A. III–V nitrides: A new age for optoelectronics. MRS Bulletin. 2003:350-353. DOI: 10.1557/mrs2003.99

[8] Holonyak N Jr. Light emitting diode birth. MRS Bulletin. 2005:509-517. DOI: 10.1557/mrs2005.5

[9] Osinski BI, et al. Optoelectronic structures based on many component semiconductors. Nauka i technika, Minsk. 1981:288 [in Russian]

[10] Akasaki I. Nitride semiconductors—Impact on the future world. Journal of Crystal Growth. 2002;**237-239**:905-911. DOI: 10.1016/S0022-0248(01)02077-2

[11] Available from: http://en.nagoya-u.ac.jp/news/nobel2014.html

[12] Nakamura S, Pearton S, Fasol G. The Blue Laser Diode. The Complete Story. New York: Springer; 2000. p. 368. DOI: 10.1007/978-3-662-04156-7

[13] Morkoc H. Handbook of Nitride Semiconductors and Devices. New Jersey: Wiley-VCH Verlag GmbH&Co; 2008. pp. 323-760. DOI: 978-3-527-62846-9

[14] Winston DW. Physical simulation of optoelectronic semiconductor devices. Colorado: University of Colorado; 1999. p. 135. Available from: http://www.simwindows.com

[15] Karpov SY, Prokofyev VG, Yakovlev EV, et al. ROLE OF GASEOUS SPECIES IN GROUP-III NITRIDE GROWTH MRS Internet Journal of Nitride Semiconductor Research. 1999;**4**:126

[16] Mymrin VF, Bulashevich KA, Podolskaya NI. Modelling study of MQW LED operation. Physica Status Solidi (c). 2005;**2**:2928-2931. DOI: 10.1002/pssc.200461289

[17] Bertolotti M, Bloemer MJ, Bowden CM, et al. Blue and green light emission: New directions and perspectives of applications of one-dimensional photonic band gap structures. Physics and Simulation of Optoelectronic Devices VIII. 2000;**3944**:680-687. DOI: 10.1117/12.391475

[18] Rozhansky IV, Zakheim DA. Analysis of the causes of the decrease in the electroluminescence efficiency of AlGaInN light-emitting-diode heterostructures at high pumping density. Semiconductors. 2006;**40**(7):861-867. DOI: 10.1134/S1063782606070190

[19] Burylova IV. Mathematical simulation of distribution of minority charge carriers, generated in multi-layer semiconducting structure by a wide electron beam. Semiconductors. 2007;**41**(4):458-461. DOI: 10.1134/S1063782607040161

[20] Zapol P, Pandey R, Gale JD. An interatomic potential study of the properties of gallium nitride. Journal of Physics: Condensed Matter. 1997;**9**:9517-9525. DOI: S0953-8984 (97)82806-8

[21] Aichoune N, Potin V, Ruteranaet P, et al. An empirical potential for the calculation of the atomic structure of extended defects in wurtzite GaN. Computational Materials Science. 2000;**17**:380-383. DOI: 10.1016/S0927-0256(00)00056-2

[22] Bere A, Serra A. Atomic structure of dislocation cores in GaN. Physical Review B. 2002;**65**:205323. DOI: 10.1103/PhysRevB.65.205323

[23] Zabelin VA, Gurevich CA. LEDS optimization. LEDs and Lasers. 2003;**1-2**:15

[24] Ambacher O, Foutz B, Smart J, et al. Two dimensional electron gases induced by spontaneous and piezoelectric polarization in undoped and doped AlGaN/GaN heterostructures. Journal of Applied Physics. 2000;**87**:334. DOI: 10.1063/1.371866

[25] Vurgaftman J, Meyer JR. Band parameters for nitrogen-containing semiconductors. Journal of Applied Physics. 2003;**94**:3675. DOI: 0.1063/1.1600519

[26] Takeuchi T, Amano H, Akasaki I. Theoretical study of orientation dependence of piezoelectric effects in wurtzite strained GaInN/GaN heterostructures and quantum wells. Japanese Journal of Applied Physics. 2000;**39**:413-416. DOI: 10.1143/JJAP.39.413

[27] Monemar B, Pozina G. Group III-nitride based hetero and quantum structures. Progress in Quantum Electronics. 2000;**24**:239-290. DOI: 10.1016/S0079-6727(00)00009-4

[28] Wetzel C, Takeuchi T, Amano H, Akasaki I. III-Nitride Semiconductors: Optical Properties. New York: Taylor & Francis; 2002. p. 291

[29] Ambacher O, Majewski J, Miskys C. Pyroelectric properties of Al(In)GaN/GaN hetero- and quantum well structures. Journal of Physics: Condensed Matter. 2002;**14**:3399-3434. DOI: 10.1088/0953-8984/14/13/302

[30] Huang X, Du C, Zhou Y, et al. Piezo-phototronic effect in a quantum well structure. ACS Nano. 2016;**10**(5):5145-5152. DOI: 10.1021/acsnano.6b00417

[31] Abramov VS, Nikiforov SG, Sushkov VP. GaN LEDs simulation. LED & Lasers. 2002;**1-2**:30-33

[32] Chichibu S, Uedono A, Onuma T, et al. Origin of defect-insensitive emission probability in In-containing (Al,In,Ga)N alloy semiconductors. Nature Materials. 2006;**5**:810. DOI: 10.1038/nmat1726

[33] Adyr FG, Simpsion TE. Nitride LED measurements. Applied Physics Letters. 2008;**93**: 023109. DOI: 10.1063/1.2992582

[34] Sg Lux GmbH Company. SiC UV Photodiodes. 2009 Available from: http://sglux.de/en/product-category/sic-uvphotodiodes/

[35] Rabinovich OI. InGaN and InGaP heterostructure simulation. Journal of Alloys and Compounds. 2014;**586**:S258. DOI: 10.1016/j.jallcom.2013.03.214

[36] Rabinovich OI, Sushkov VP. The study of specific features of working characteristics of multicomponent heterostructures and AlInGaN-based light-emitting diodes. Semiconductors. 2009;**43**(4):524. DOI: 10.1134/S1063782609040228

[37] Rabinovich O, Legotin S, Didenko S, et al. Heterostructure optimization for increasing LED efficiency. Japanese Journal of Applied Physics. 2016;**55**:05FJ131. DOI: 10.7567/JJAP.55.05FJ13

[38] Yang W, et al. Phototransistor. Patent No. US006137123A, October 24, 2000

[39] Sushkov VP, Vigdorovich EN. Abstracts IV. Russian-Japanese Workshop; 4-16 July 2006; **2**:659

[40] Rabinovich OI. Quantum yield of LEDs based on InGaN/GaN structures at silicon substrates. Light & Engineering. 2013;**21**(2):78-82

[41] Rabinovich OI. Compound semiconductor materials and devices. III-nitride optical devices. SPIE, Bellinghain. Vol. 1635. In: Materials Research Society Fall Meeting 2013, Symposium T; 2-4 December 2013; Boston, MA, USA. pp. 15-22. DOI: 10.1557/opl.2014.336

[42] Rabinovich OI, Legotin SA, Didenko SI. Impurity influence on nitride LEDs. Journal of Nano and Electronic Physics. 2014; **6**(3):030021-030022

[43] Rabinovich OI, Didenko S, Legotin S. Nitride heterostructure influence on efficiency droop. SPIE, Bellinghain In: Proceedings of SPIE, Vol. 9383. Light-Emitting Diodes: Research, Manufacturingand Application for Solid State Lighting XIX; 2-10 February 2015; San Francisco,California, USA. pp. 938310-1-938310-6. DOI: 10.1117/12.2078317